ELECTROOSMOTIC INTERFACIAL ADHESION FORCES BETWEEN UNSATURATED SOIL AND METALS
/
基于电渗的非饱和土壤与金属界面粘附力研究

Xin ZHENG*[1,2)], Junxiang HAO[1)], Hengyan XIE[1,2)], Wenbao XU[2]
[1)] College of Engineering, Heilongjiang Bayi Agricultural University, Daqing / China;
[2)] College of Civil Engineering and Water Conservancy, Heilongjiang Bayi Agricultural University, Daqing / China;
Corresponding author: Xin ZHENG; *Tel: +86 13059051417; E-mail: zhxin@byau.edu.cn*
DOI: https://doi.org/10.35633/inmateh-78-06

Keywords: *Electroosmosis*; *Unsaturated soil*; *Metal-interface adhesion force*; *Adhesion reduction mechanism*

ABSTRACT
Soil adhesion markedly increases operational resistance, diminishes efficiency, and elevates energy consumption in the soil contact components of agricultural machinery. This study introduces a method for reducing adhesion and facilitating detachment through electroosmosis, while also examining its effects on energy consumption via pull-out and slip tests. The results indicate that electroosmosis generates a water film at the metal interface, which significantly decreases the interfacial adhesion force. At 60 V and a soil moisture content of 30%, the pull-out force is reduced by 21.48 N, and the slip angle decreases by 55.8°. Compared to traditional methods, electroosmosis not only lowers energy consumption but also effectively mitigates wear and maintenance costs.

摘要
土壤与农机触土部件间的粘附作用会显著增大作业阻力、降低工作效率、增加能源消耗，进而影响作业质量。本文通过拉拔、滑移试验分析不同金属材料与不同含水率土壤接触时的电渗效应以及能量消耗分析提出了一种基于电渗技术的减粘脱附方法。结果表明：电渗作用能引导土壤水分向阴极迁移，在金属界面形成润滑水膜，从而显著降低界面粘附力；在电压 60V、土壤含水率 30%的条件下，铜界面的拉拔力降低 21.48N，滑移角下降 55.8°。与传统减粘方法相比，电渗技术能耗更低，并能有效减少农机设备的磨损与维护成本，为触土部件的设计与性能优化提供了新的技术途径。

INTRODUCTION

The adhesion between agricultural machinery soil contact components and soil increases operational resistance, reduces work efficiency, and raises energy consumption. Existing studies indicate that soil adhesion increases plowing resistance by over 30%, causes a 30%-50% rise in energy consumption for tillage machinery, and decreases the production efficiency of seeding machinery by 30% *(Li et al., 2022; Qiu et al., 2020; Tjandra et al., 1979)*.

Researchers in agricultural engineering have focused on adhesion reduction measures to mitigate the negative effects of soil-interface contact and relative motion on machine performance and efficiency *(Cui et al., 2023; Fang et al., 2024)*.

Theoretical models suggest that changes in soil moisture content alter the water film at the contact surface, which impacts the adsorption force on soil particles and, consequently, the interfacial adhesion force *(Hashemi et al., 2023; Qiu et al., 2020)*. Experimental data show that as soil moisture content increases, the adhesion force initially increases before decreasing *(Khan et al., 2010; Tong et al., 1994)*.

Various adhesion reduction methods, including mechanical, surface modification, electroosmotic, and heating-based techniques, have been explored (*Stenberg et al., 2000; Sun et al., 2020*). *Li et al. (2022)* found that the interaction between soil particle size distribution and moisture content influences adhesion force, and emphasized that the structure and water absorption capacity of soil particles are the key factors determining adhesion force.

Tjandra et al. (1979) and *Zhang et al. (2022)* noted that excessive moisture leads to soil expansion, reducing friction and affecting pile load-bearing capacity. Relevant literature indicates that the adhesion force between soil and contact components is significantly correlated with moisture content. Specifically, adhesion initially increases and subsequently decreases as moisture content rises. This trend can be attributed to alterations in the state of the interfacial water film.

When moisture content is either too low or too high, adhesion diminishes due to the discontinuity of the water film or excessive lubrication resulting from an overly thick film, respectively *(Asadi et al., 2013; Wang et al., 2021; Dai et al., 2013)*. *Cong et al. (1990)* conducted an application study on electroosmotic soil detachment, performing a comprehensive and systematic experimental investigation of factors affecting electroosmotic adhesion reduction effects, such as electroosmotic time, electroosmotic voltage, and soil moisture content, revealing the regularity and nature of their influence on electroosmotic effects. Based on extensive experiments, a mathematical model was developed to describe the relationship between electroosmotic energy consumption and soil adhesion force *(Patel et al., 2021; Sun et al., 2012)*. Electroosmotic technology has significant guiding implications for the design of soil contact surface structures and materials, as it can optimize the contact mechanics characteristics between components and soil *(Abbaspour-Gilandeh et al., 2018; Xu et al., 2024)*.

However, despite the application of electroosmotic technology in other fields, systematic research on its application in agricultural machinery adhesion reduction remains limited, particularly regarding the electroosmotic effects on different metal interfaces and the impact of varying soil moisture content on adhesion force. This paper conducts a systematic experimental study to explore the adhesion reduction mechanism based on electroosmotic technology and analyze the electrokinetic behavior between different metal materials and soil under the influence of electroosmosis. It aims to provide new technological insights for the design of agricultural machinery soil contact components, promote the application of electroosmosis in agricultural machinery, and ultimately enhance operational efficiency, reduce energy consumption, and optimize the contact mechanics properties between soil and agricultural machinery soil contact components. This research presents a new technological approach for adhesion reduction in agricultural machinery design.

MATERIALS AND METHODS

Preparation of Clay Specimens and Interfacial Materials

The soil utilized in this study was sourced from the tillage layer of Heshan Farm, located within the Jiusan Administration of Heilongjiang Province. The soil samples underwent natural air-drying indoors, followed by crushing and sieving through a 0.2 mm standard sieve to eliminate coarse particles that could compromise interfacial homogeneity. In accordance with the Standard for Geotechnical Testing Methods (GB/T 50123-2019), the fundamental physical indices of the undisturbed soil were assessed using an LP-100D liquid-plastic limit combined tester. The findings are summarized in Table 1.

Table 1

Basic physical properties of soil samples

Soil	Specific gravity	Permeability coefficient (cm/s)	Liquid limit (%)	Plastic limit (%)
Clay soil	2.97	3.2×10^{-7}	29.4	16.7

Four distinct types of test soil specimens were prepared with volumetric water contents of 15%, 20%, 25%, and 30%, employing a 125D-1CN precision electronic balance with an accuracy of 0.01 g. The uniformly mixed soil specimens were subsequently placed in a JYH-40B constant temperature and humidity curing chamber, maintained at a temperature of 25± 1°C and a relative humidity of 60± 5%. They were allowed to equilibrate for 48 hours to ensure thorough and uniform moisture diffusion. All tests were conducted within the aforementioned constant temperature and humidity environment (25±2°C, 50± 5% relative humidity) to mitigate the effects of environmental fluctuations.

The soil container was custom-fabricated from transparent acrylic, featuring internal dimensions of 300 mm (length)× 200 mm (width)× 150 mm (height) and a wall thickness of 5 mm. Three commonly utilized agricultural machinery metals were selected: stainless steel (grade 304), copper (grade T2), and mild steel (grade Q235). All test plates were uniformly processed to dimensions of 160 mm (length)× 80 mm (width)× 3 mm (thickness). To maintain consistent surface conditions, the specimens' surfaces were ground with 60-grit sandpaper, achieving a final arithmetic mean roughness controlled within the range of 0.8± 0.1 μm, as measured using a handheld roughness tester (SJ-210).

Design of Pull-out Test Method

The pull-out test is designed to quantify the normal adhesion force at the soil–metal interface. The test setup is illustrated in Fig. 1. It was conducted using an Instron 5967 universal testing machine, which has a maximum load capacity of 10 KN and a displacement resolution of 0.001 mm.

The procedure involved several steps: Initially, the prepared soil was placed into a custom soil container and compacted in layers with a 2.5 kg standard Proctor hammer. Each soil layer, approximately 30 mm thick, received 25 blows for compaction, and the surface was leveled using a scraper. The conical indenter, attached to the testing machine (with a tip angle of 30°, a height of 20 mm, and a base diameter of 10.7 mm), was subsequently driven vertically into the soil sample at a constant rate of 2 mm/min until a depth of 10 mm was attained. The load was then held for 60 s to allow the soil stress distribution to stabilize. Immediately following the holding period, the test plate was pulled vertically upward at the same rate. Force–displacement curves were recorded simultaneously during the pull-out process, with the peak pull-out force representing the interfacial normal adhesion force. Each test group was repeated three times, and the average of the results was taken as the final outcome.

Slip Angle Test Method

The slip angle test assesses the tangential adhesion characteristics and critical slip conditions at the soil–metal interface. The test setup is illustrated in Fig. 2. It was conducted on a self-constructed inclined platform measuring 500 mm × 300 mm. The inclination angle of the platform is adjusted using an electric telescopic rod driven by a 57BYG stepper motor, with direct measurements taken by a mechanical high-precision inclinometer, achieving an angle measurement accuracy of ±0.1°. For the test, the cured soil sample is initially placed into a mold and uniformly compacted using a 2.5 kg Proctor hammer. The surface is leveled prior to demolding to create the specimen. Subsequently, the specimen is positioned at the center of a horizontally oriented metal test plate, onto which a 2.5 kg standard weight is applied for 60 s to ensure uniform interfacial contact. After pre-compression, the weight is removed, and the test plate with the specimen is promptly mounted onto the inclined platform. The control system is activated to tilt the platform at a constant angular velocity of 0.5°/s. The inclination angle at which the specimen begins to slide continuously and steadily is recorded as the critical slip angle. Each test group is repeated three times, with the average value of the results taken as the final outcome.

Electroosmosis Test Method

To systematically examine the impact of electroosmosis on adhesion behavior at the soil–metal interface, three types of electroosmosis tests were conducted by integrating an electric field into the pull-out and slip angle test methodologies. All tests utilized a consistent configuration: the conical indenter and the metal test plate functioned as the cathode, while a stainless-steel plate (60 mm × 80 mm × 3 mm) was positioned parallel to the soil specimen as the anode. A Rigol DP832A programmable DC power supply, characterized by a voltage accuracy of ± (0.05% + 3 mV) and a maximum current output of 3 A per channel, was utilized to deliver predetermined voltages of 30 V, 45 V, and 60 V. Concurrently, a UNI-T UT61E digital multimeter monitored the circuit current in real time, facilitating subsequent analysis of energy consumption. In the electroosmotic pull-out test, the power supply was activated during the load-holding phase of the conventional pull-out procedure. Following 60 seconds of continuous electrification, the pull-out was conducted immediately, and the normal adhesion force after electroosmosis was recorded. The soil's electrical conductivity was measured before and after the test using an HI98331 conductivity meter, and variations in soil temperature were monitored. The electroosmotic slip angle test was developed to investigate the influence of the electric field on tangential adhesion characteristics. Following the pre-compression of the specimen, the anode plate was positioned, and the designated voltage was applied. While maintaining the voltage, the platform inclination was increased at a rate of 0.5 °/s. The critical slip angle, at which the specimen began to slide continuously under the sustained electric field, was recorded and compared to the condition without an electric field. Additionally, to assess the response speed of interface detachment induced by electroosmosis, an electroosmotic slip time test was performed. The platform inclination was fixed at 30 °, and after installation, the specified voltage was applied to the specimen. A stopwatch recorded the time elapsed from power-on to the onset of sliding, thereby characterizing the dynamic process of interface state alteration under electroosmosis. Each test group was repeated three times, and the average value was taken as the final result. Schematic diagrams of the electroosmosis tests are presented in Fig. 1 and Fig. 2.

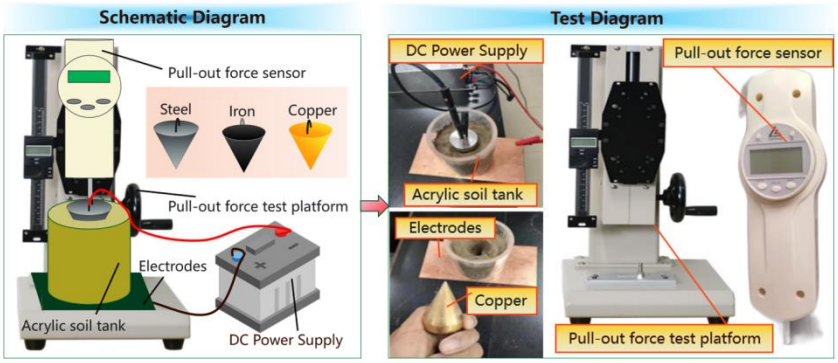

Fig. 1 - Pulling test apparatus

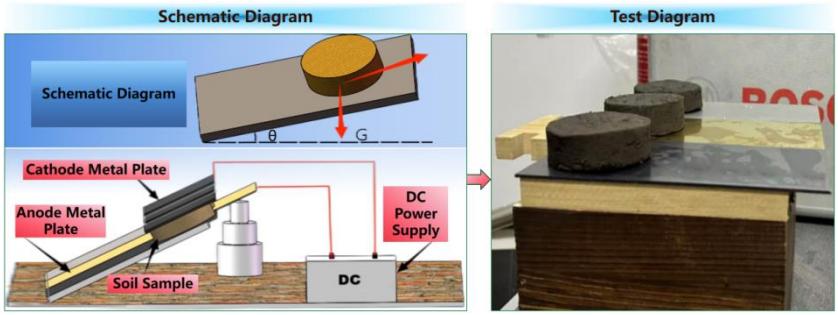

Fig. 2 - slope test device

RESULTS

Pull-out Test Results

Effect of Moisture Content on Soil-Interface Adhesion Force

The pull-out forces for different metal interfaces were measured using the test setup shown in Fig. 1, as depicted in Fig. 3.

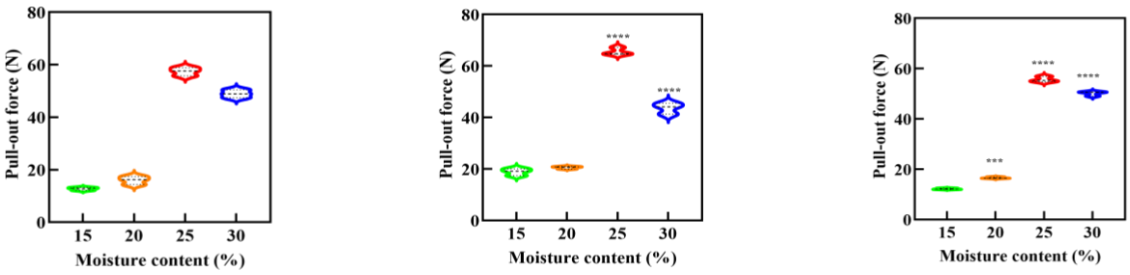

a) *b)* *c)*

Fig. 3 - Pull-out forces for different metal interfaces

a) Steel Interface. b) Iron Interface. c) Copper Interface

As shown in Fig. 3, the interfacial adhesion force between the soil and different metals increases initially and then decreases as the soil moisture content rises. The maximum adhesion force is observed at a moisture content of 25%, indicating that the effect of moisture content on adhesion is most significant at this point. As the moisture content approaches the liquid limit, the adhesion force between the soil and metal surfaces gradually weakens. This suggests that the adhesion phenomenon of agricultural machinery soil contact components predominantly occurs in the unsaturated zone. At a moisture content of 25%, the adhesion force between the soil and the contact components is at its highest, with the adhesion force at the iron interface being the strongest, and the adhesion force at the copper interface being the weakest. The difference in adhesion forces between the iron and copper interfaces shows significant variation under different moisture contents, with the largest difference of 9.9 N occurring at a moisture content of 25%, and the smallest difference of 1.96 N occurring at a moisture content of 20%.

Analysis of Electroosmotic Effect

The electroosmotic effect comparison test results are shown in Fig. 4.

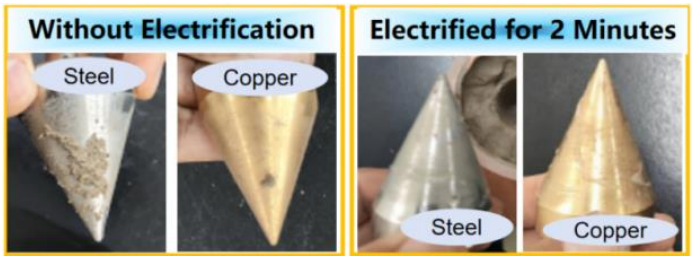

Fig. 4 - Electroosmotic effect comparison analysis

The pull-out force test results for different metal interfaces under various moisture contents, after applying the electroosmotic effect, are shown in Fig. 5.

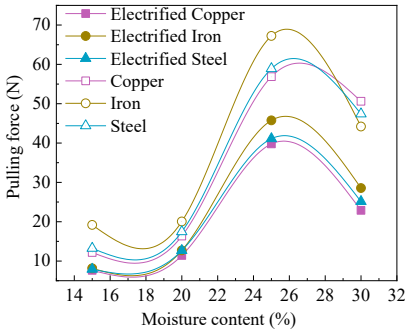

Fig. 5 - Metal-interface adhesion forces at different moisture contents

As seen from Fig. 4 and Fig. 5, under the same conditions, applying an electric current causes water in the soil to migrate directionally towards the cathode surface, forming a water film at the soil-metal interface. This leads to a significant reduction in the adhesion force due to the change in moisture content at the contact zone. This demonstrates that applying an electric current can alter the distribution of moisture at the contact surface, thus reducing soil adhesion, especially when the moisture content is 25%. After applying current for 1 minute, a distinct water film forms between the metal and the soil contact zone. The thickened water film plays a significant lubricating role, reducing soil adhesion. After electroosmosis, the pull-out force at a moisture content of 25% decreases most noticeably by 21.48 N. This also confirms the conclusion by Ren Luquan's team *(Martin, 2019)* that the moisture migration induced by electric potential leads to an uneven distribution of moisture in the soil, transitioning the adhesion between the soil and the contact component from frictional behavior to lubrication.

Slope Shear Test Results

Shear Angle of Soil Samples under Different Metal Interfaces and Moisture Content Conditions

The shear angles of soil samples with different moisture contents and materials are shown in Fig. 6.

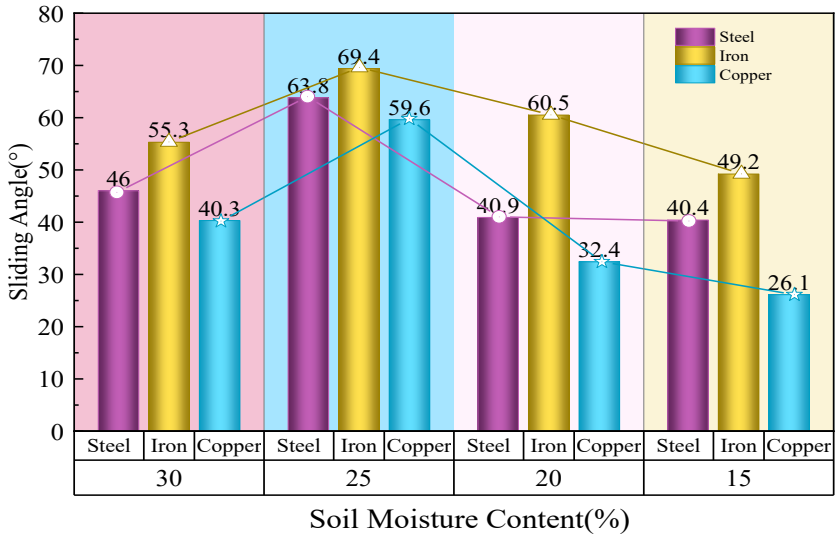

Fig. 6 - Shear angles of different materials at various moisture contents

As shown in Fig. 6, there are significant differences in the shear angles of soil samples with different metal materials. Taking a soil moisture content of 30% as an example, the shear angle at the copper interface is the smallest, exhibiting the best shear detachment performance. The shear angle at the steel interface is slightly larger than at the copper interface, with an increase of 5.7°, while the shear angle at the iron interface is the largest, exceeding the copper interface by 15°. This indicates that there are differences in the friction coefficients between different metal interfaces, leading to variations in the shear angles of the soil samples. Moreover, the soil moisture content significantly affects the interfacial adhesion force between the soil and the metal interfaces. For the steel interface, when the soil moisture content is 25%, the adhesion force between the soil and the metal interface reaches its maximum value, with a shear angle of 63.8°. This shows that as the moisture content approaches the liquid limit, the adhesion force between the soil and the metal surface increases. However, once the moisture content exceeds the liquid limit, the adhesion force starts to decrease. Therefore, without the influence of an electric field, the shear angle and adhesion force are jointly affected by the metal interface characteristics and the soil moisture content.

Changes in Shear Angle under Different Voltages, Moisture Contents, and Metal Interfaces

The voltage is taken as the independent variable on the x-axis, soil moisture content as the independent variable on the y-axis, and the shear angle as the dependent variable on the z-axis. A bar chart of the shear angles at the copper interface, iron interface, and steel interface was drawn, and the fitting relationship between the shear angle of the soil sample at each metal interface and voltage and moisture content was derived through surface fitting. The changes in shear angles at different metal interfaces under different voltage and moisture content conditions are shown in Fig. 7.

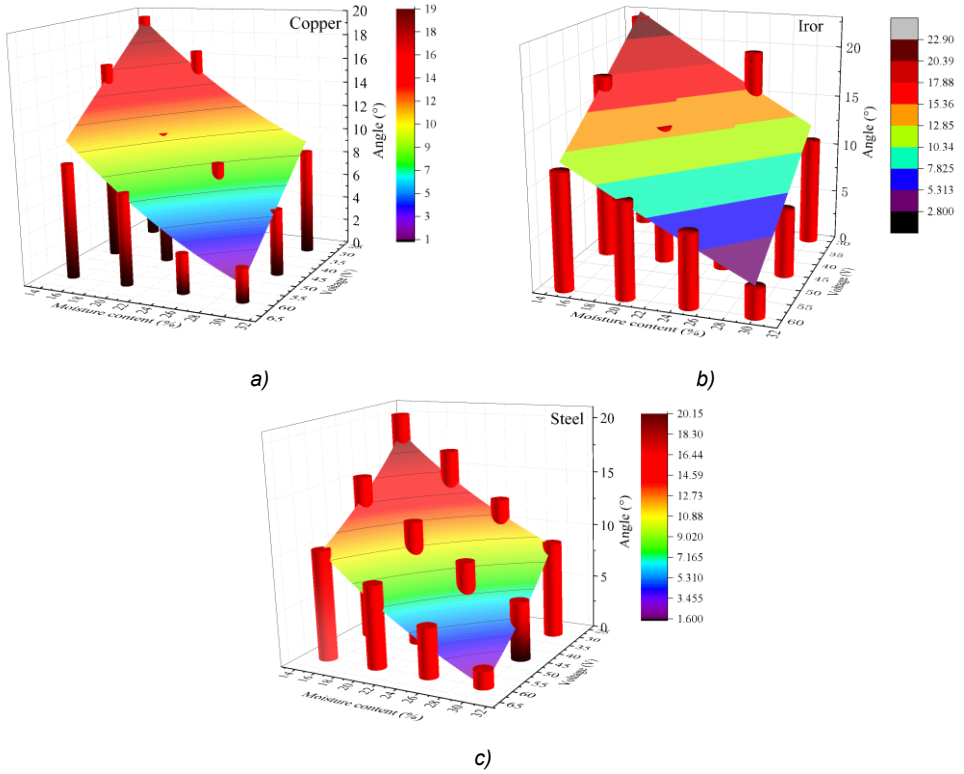

Fig. 7 - Shear angle at different metal interfaces under varying voltage and moisture content conditions

a) Copper interface shear angle. b) Iron interface shear angle. c) Steel interface shear angle

Fig. 7 presents the shear angles of soil samples on various metal interfaces. The figure includes bar charts illustrating shear angles for the copper interface (Fig. 7a), iron interface (Fig. 7b), and steel interface (Fig. 7c), along with corresponding fitted equations derived from surface fitting. From Fig. 7a and Fig. 7c, it is evident that within the voltage range of 30 V to 60 V, the shear angles of soil samples on copper and steel interfaces exhibit concave surface profiles. This observation indicates a rapid voltage drop, suggesting that these interfaces are particularly sensitive to voltage variations. Under consistent water content conditions, the shear angle decreases progressively as the voltage increases, indicating that higher voltages promote the acceleration of water film formation. Notably, under steel interface conditions with a soil water content of 15 % and a voltage of 60 V, the shear angle of the soil sample reaches 10.2 °, outperforming other combinations.

Additionally, an increase in water content positively influences the shear angle; for example, at 60 V, the shear angle for a soil sample with 30 % water content is only 1.6 °, demonstrating that water film formation is affected by both voltage and water content. Fig. 7b illustrates that for the iron interface, within the same voltage range of 30 V to 60 V, the shear angles of soil samples exhibit a convex surface profile. The iron interface demonstrates reduced sensitivity to voltage; even as voltage increases, the shear angle remains comparatively large. Likewise, an increase in water content results in a decrease in the shear angle.

By comparing Fig. 7a, Fig. 7b, and Fig. 7c, it can be seen that the shear angle of soil samples at the copper interface changes little after electrification compared to the steel and iron interfaces. This may be related to the stronger hydrophilicity of the copper interface. Copper interfaces have stronger hydrophilicity, which allows them to adsorb water molecules more easily, promoting the formation of a water film and reducing friction.

To investigate the influence of moisture content and voltage on the shear time of soil samples under different metal interface conditions, a bar chart of the shear time was plotted with voltage as the x-axis, moisture content as the y-axis, and shear time as the z-axis. The fitting model for the shear angles of the soil samples at the copper, iron, and steel interfaces with respect to voltage and moisture content were derived through surface fitting, as shown in Fig. 8.

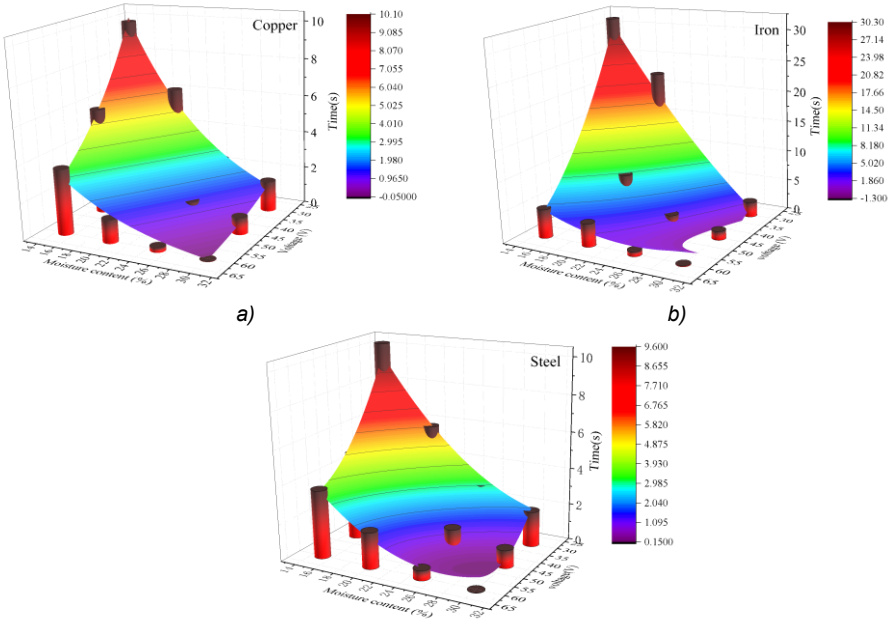

Fig. 8 - Shear time under different voltage and moisture content conditions at different metal interfaces

a) Copper interface shear time. b) Iron interface shear time. c) Steel interface shear time

As shown in Fig. 8, the shear time for the three metal interfaces decreases as the voltage and moisture content increase. Applying electroosmosis to reduce the adhesion between clay and the metal interface requires certain voltage conditions. When the voltage applied to the soil sample is low, the shear time is longer. This is because under low voltage and low moisture content conditions, water migration is insufficient, and the water film between the soil and metal interface is not thick enough to overcome the static friction, thus failing to achieve the electroosmotic adhesion reduction effect. When the voltage is lower than the detachment voltage threshold, water migration from the anode to the cathode is slow, and the formation of the water film is also slow, resulting in a prolonged shear time. Once the voltage reaches the detachment threshold, water migrates faster from the anode to the cathode and forms a water film at the cathode interface, preventing adhesion and causing the sample to start sliding. As the applied voltage increases, the formation speed of the water film at the cathode metal interface increases, and the soil sample detachment time significantly shortens. However, as the voltage further increases, especially when it exceeds 60 V, the influence of increased voltage on the shear time gradually diminishes, and the detachment time tends to stabilize at around 0.1 seconds. The difficulty of soil detachment is positively correlated with moisture content. At a voltage of 45 V, the copper interface is the easiest to detach at a moisture content of 30%, while as the moisture content decreases, the detachment difficulty significantly increases. Surface fitting analysis shows that the shear time for the three metal interfaces exhibits a concave cylindrical shape, indicating that the effects of moisture content and voltage on shear time are significant. Under a voltage of 60 V and moisture content of 30%, the shear time reaches its minimum value, approximately 0.1 seconds.

Energy Consumption

Theoretical Basis

Energy consumption is a crucial factor in applying electroosmosis technology to solve soil adhesion issues. Compared to other methods, electroosmotic adhesion reduction has the advantage of uniformly treating large areas of soil, reducing wear and maintenance costs for mechanical equipment, and keeping energy consumption within a controllable range. The energy required for the soil sample to start sliding after the applied voltage is defined as the effective energy consumption, as shown in Equation (1).

$$E = P \cdot t \tag{1}$$

where: E is the effective energy consumption (J); P is the power during the sliding process (W); t is the time taken for sliding to begin (s).

For a direct current power supply, the power consumption is given by Equation (2).

$$P_{dc} = U \cdot I \tag{2}$$

where: U is the voltage (V); I is the current intensity (A).

Effective energy consumption analysis

The purpose of energy consumption measurement is to identify the optimal parameters for energy consumption under the electroosmotic effect and to explore the influence of various factors on energy consumption. Based on the Box-Behnken Design in the Design-Expert software, the effective energy consumption from the slope shear test under the electroosmotic effect was analyzed.

The results of the variance analysis for effective energy consumption, obtained through Design-Expert software, are presented in Table 2. A second-order multiple regression fitting was performed on the data in Table 2, yielding the second-order regression equation for effective energy consumption in relation to the coded independent variables, as expressed in Equation (3).

$$Y = 2.39 + 0.069A + 0.081B + 0.003C - 0.053AB + 0.048AC - 0.012BC + 0.5A^2 + 0.25B^2 + 0.29C^2 \tag{3}$$

Table 2

Variance Analysis of Effective Energy Consumption

Source of Variation	Sum of Squares	Degrees of Freedom	Mean Square	F-value	P-value
Model	1.96	9	0.22	603.88	0.0001
A - Voltage	0.038	1	0.038	104.61	0.0001
B - Moisture Content	0.052	1	0.052	145.21	0.0001
C - Angle	5×10^{-5}	1	5×10^{-5}	0.14	0.721
AB	0.011	1	0.011	30.79	0.0009
AC	9.1×10^{-3}	1	9.1×10^{-3}	25.23	0.0015
BC	5.5×10^{-4}	1	5.5×10^{-4}	1.53	0.2563
A^2	1.07	1	1.07	2959.85	0.0001
B^2	0.27	1	0.27	743.12	0.0001
C^2	0.34	1	0.34	949.99	0.0001
Lack of Fit	1.17×10^{-3}	3	3.92×10^{-4}	1.16	0.4293
Pure Error	1.36×10^{-3}	4	3.39×10^{-4}		
Total	1.97	16			

Based on the variance analysis results in Table 2, it can be concluded that the factors A, B, AB, AC, A^2, B^2, and C^2 are highly significant, while other factors are not significant. The p-value for the lack of fit is 0.4293, which is clearly greater than 0.05, indicating a high degree of fit for the quadratic multiple regression model, with no lack of fit factors present. This model can replace the experimental data points for analysis. Furthermore, the significance order of the factors affecting the effective energy consumption, from largest to smallest, is as follows: soil moisture content, voltage, and angle.

A response surface analysis for effective energy consumption was conducted, and through Design-Expert analysis, it was found that the significant interaction terms AB and AC affect the response surface and contour plot for effective energy consumption, as shown in Fig. 9.

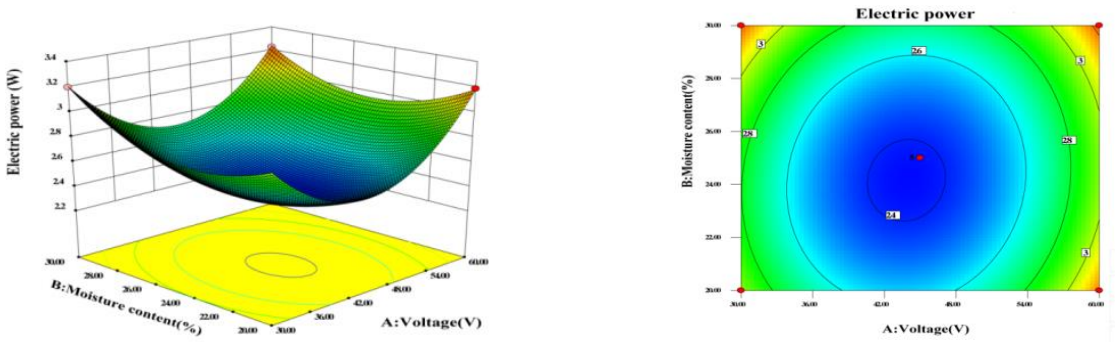

a) *b)*

Fig. 9 - Interaction response plot of voltage and moisture content

a) Response surface plot. b) Contour plot

From Fig. 9, it can be observed that within the experimental data space, as voltage and soil moisture content increase, the time for soil sample slip decreases, and the effective energy consumption decreases with their increase. The effective energy consumption follows a trend of first decreasing and then increasing with the increase in depression, indicating that with the increase in voltage and soil moisture content, once the slip time of the soil sample no longer decreases, it leads to an increase in effective energy consumption. The shape of the contour lines reflects the significance of the interaction between the two factors. From the figure, it is evident that the AB interaction significantly affects effective energy consumption.

The interaction response plot for voltage and angle is shown in Fig. 10.

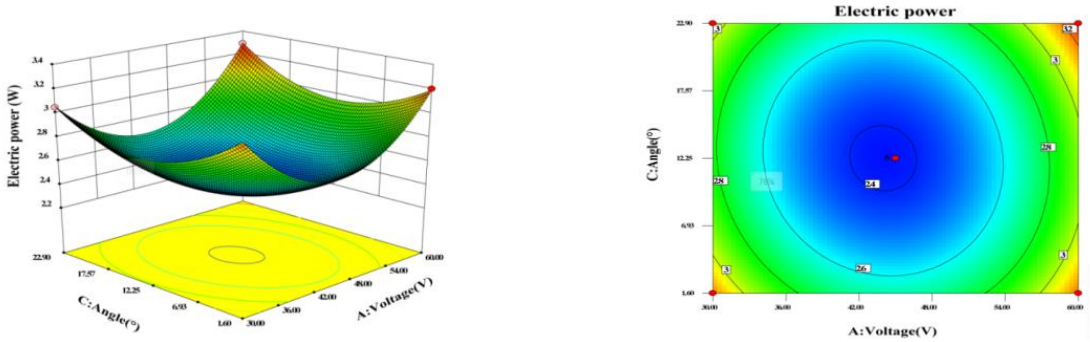

a) *b)*

Fig. 10 - Interaction response plot of voltage and angle

a) Response surface plot b) Contour plot

As shown in Fig. 10, within the test data space, as the voltage and angle increase, the soil sample slides faster, and the effective energy consumption decreases with the increase of both factors. However, when the voltage and angle increase to a certain threshold, the difference in power under different voltages gradually diminishes, indicating that further increases in voltage have a diminishing effect on power. This suggests that under high voltage conditions, the electroosmotic effect reaches saturation, and the power increase slows down. The shape of the contour lines reflects the significance of the interaction between the two factors. It can be observed that the AC interaction significantly affects effective energy consumption. The above analysis is consistent with the significance shown in Equation (3).

The optimization model and the experimental verification

Based on the actual operational demands for adhesion reduction in agricultural machinery soil-engaging components, this study aims to achieve effective detachment while maintaining lower energy consumption. Accordingly, effective energy consumption was defined as the objective function for optimization, with 3 key experimental parameters—voltage, soil moisture content, and inclination angle—selected as the design variables for systematic optimization.

The optimization was performed using Design-Expert software, yielding the following optimal parameter combination for minimizing energy consumption: voltage 43.84 V, moisture content 24.15 %, and inclination angle 12.24°.

To facilitate practical application in field operations, the optimized parameters were rounded to the following practical values: voltage 44 V, moisture content 24 %, and inclination angle 12°, 3 repeated verification tests were conducted under these rounded conditions, resulting in an average effective energy consumption that closely matched the predicted optimum, thereby confirming the reliability and validity of the established regression model.

CONCLUSIONS

This paper systematically investigates the variation patterns of adhesion forces at the interface between unsaturated soil and metals under the influence of electroosmotic effects, utilizing pull-out and slip tests. The findings indicate that electroosmosis technology can significantly reduce interfacial adhesion and optimize energy consumption characteristics, thereby providing a solid technical foundation for the anti-adhesion design of soil-engaging components in agricultural machinery.

(1) Electroosmosis markedly diminishes adhesion by directing water migration toward the cathode, which results in the formation of a continuous lubricating water film at the metal interface. Soil moisture content initially increases before decreasing in correlation with adhesion force, peaking at 25% moisture content. Under electroosmotic treatment at 60 V and 30% moisture content, the pull-out force at the copper interface decreased by 21.48 N, while the slip angle was reduced by 55.8°.

(2) Different metal interfaces exhibit significant variations in their responses to electroosmotic adhesion reduction. Copper, characterized by its strong surface hydrophilicity, facilitates water film formation and demonstrates the most effective anti-adhesion effect. Both voltage and moisture content jointly influence slip behavior, with the shortest slip time (approximately 0.1 s) occurring at 60 V and 30% moisture content, indicating that electroosmosis effectively promotes the transition of the interface state from friction to lubrication.

(3) Utilizing the Box-Behnken experimental design and response surface analysis, a regression model was developed to characterize the relationship among voltage, moisture content, inclination angle, and effective energy consumption. The optimal parameters identified for minimizing energy consumption were: voltage 43.84 V, moisture content 24.15%, and inclination angle 12.24°. In comparison to conventional methods, electroosmotic adhesion reduction technology exhibits reduced energy consumption while also demonstrating strong engineering applicability and economic efficiency.

ACKNOWLEDGEMENT

This research was funded by Supported by Heilongjiang Provincial Natural Science Foundation of China (PL2024E024).

REFERENCES

[1] Asadi, A., Huat, B.B.K., Nahazanan, H., Keykhah, H.A., (2013). Theory of electroosmosis in soil. *Int. J. Electrochem*. Sci. 8, 1016–1025.

[2] Abbaspour-Gilandeh, Y., Hasankhani-Ghavam, F., Shahgoli, G., Shrabian, V.R., Abbaspour-Gilandeh, M., (2018). Investigation of the effect of soil moisture content, contact surface material and soil texture on soil friction and soil adhesion coefficients. *Acta Technol. Agric*. 21, 44–50.

[3] Cong Xi, Ren Luquan, Chen Bingcong, (1990). Application research on electric osmosis desulfurization of soil by earthmoving machinery. *Engineering Machinery. 21, 22-26+52*.

[4] Cui, J., Xu, G., Fang, Y., Chen, Z., Yao, Z., Tao, L., Qu, L., (2023). Experimental assessment of soil/metal interface adhesion behaviours of EPB shield machines. *Tunnelling Underground Space Technol*. 131, 104835.

[5] Dai Binggui, Chen Wengang, Li Zuyang, Zhang Yao, Yang Xiaodong, Zhang Jihao, (2025). Research Progress on Bionic Anti-Resistance Grinding Characteristics of Agricultural Soil-Contact Tools. *Journal of Agricultural Machinery in China*, 46, 45–53.

[6] Fang, Y., Zhuo, B., Zhang, R., Wang, Y., Dou, L., Yao, Y., (2024). Soil conditioning of clay based on interface adhesion mechanism: Microscopic simulation and laboratory experiment. *Underground Space*, 18, 239–255.

[7] Hashemi, A., Sutman, M., Medero, G.M., (2023). A review on the thermo-hydro-mechanical response of soil–structure interface for energy geostructures applications. Geomech. Energy Environ. 33, 100439.

[8] Khan, Muhammad, Azam, Qaisrani, Rashid, Jian-qiao, L.I., (2010). The techniques of reducing adhesion and scouring soil by bionic -- review of literature. *Adv. Nat. Sci,* 3, 41-50.

[9] Li, H., Zhang, Z., Zhai, J., Yang, L., Long, H., (2022). Correlation between soil structural parameters and soil adhesion based on water film theory. *Coatings*, 12, 1743.

[10] Patel, S.K., Biesheuvel, P.M., Elimelech, M., (2021). Energy consumption of brackish water desalination: Identifying the sweet spots for electrodialysis and reverse osmosis. *ACS Es&t Eng*. 1, 851–864.

[11] Qiu, T., Liu, C., Zhong, X., Zhu, Y., (2020). Experimental research on the impact of temperature on the adhesion characteristics of soil-structure interface. *Geofluids*, 1–9.

[12] Stenberg, M., Stenberg, B., Rydberg, T., (2000). Effects of reduced tillage and liming on microbial activity and soil properties in a weakly-structured soil. *Appl. Soil Ecol*. 14, 135–145.

[13] Sun, T.R., Ottosen, L.M., (2012). Effects of pulse current on energy consumption and removal of heavy metals during electrodialytic soil remediation. *Electrochim. Acta,* 86, 28–35.

[14] Sun, J., Wang, Y., Zhang, S., Ma, Y., Tong, J., Zhang, Z., (2020). The mechanism of resistance-reducing/anti-adhesion and its application on biomimetic disc furrow opener. *Math. Biosci. Eng*, 17, 4657–4677.

[15] Tjandra, D., Indarto, Soemitro, R.A.A., (1979). The effects of water content variation on adhesion factor of pile foundation in expansive soil. *Civ. Eng. Dimens.*, 15, 114–119.

[16] Tong, J., Ren, L., Chen, B., Qaisrani, A.R., (1994). Characteristics of adhesion between soil and solid surfaces. *J. Terramech*., 31, 93–105.

[17] Wang, L.J., Wang, Y.M., Liu, S.H., Huang, P.H., (2021). Analytical investigation of electroosmotic consolidation in unsaturated soils considering the coupling effect and a nonuniform initial water content. *Int. J. Geomech*., 21, 6021018.

[18] Xu, Z., Qi, H., Gao, P., Wang, S., Liu, X., Ma, Y., (2024). Biomimetic design of soil-engaging components: A review. *Biomimetics*, 9, 358.

[19] Martin L., Alizadeh V., Meegoda J., (2019). Electro-osmosis treatment techniques and their effect on dewatering of soils, sediments, and sludge: A review. *Soils and Foundations*. 59(2), 407-418.

[20] Zhang, L., Hu, L., (2022). Numerical simulation of electro-osmotic consolidation considering tempo-spatial variation of soil pH and soil parameters. *Comput. Geotech*. 147, 104802.